ORIGINAL ARTICLE

Accuracy of cone-beam computed tomography imaging of the temporomandibular joint: Comparisons with panoramic radiology and linear tomography

Oana Bida Honey,[a] William Charles Scarfe,[b] Michael J. Hilgers,[c] Kathleen Klueber,[d] Anibal M. Silveira,[e] Bruce S. Haskell,[f] and Allan G. Farman[g]

Louisville, Ky

Introduction: Cone-beam computed tomography (CBCT) is increasingly being used as an imaging modality, particularly in the assessment of the temporomandibular joint (TMJ). A blinded observational cross-sectional in-vitro study was conducted to compare the diagnostic accuracy of observers viewing images made with CBCT, panoramic radiography, and linear tomography. The task was to detect cortical erosions affecting the mandibular condylar head. **Methods:** The sample consisted of 37 TMJ articulations from 30 skulls with either normal condylar morphology (n = 19) or erosion of the lateral pole (n = 18). The articulations were imaged by using corrected angle linear tomography (TOMO), normal (Pan-N) and TMJ-specific (Pan-TM) panoramic radiography, and CBCT. Digital images were obtained with photostimulable phosphor plates for all modalities except CBCT. The CBCT detector used an amorphous silicon flat-panel array combined with cesium iodide. Images and 10 rereads were presented to 10 observers on a flat-panel display at a pixel-to-monitor ratio of 1:1. CBCT multi-planar images were presented both statically (CBCT-S) and interactively (CBCT-I). The observers were permitted to scroll through axial (0.4 mm) and para-sagittal (1 mm) sections and then independently rate their confidence about the presence or absence of cortical erosion. Intraobserver reliability was determined by weighted kappa and diagnostic accuracy by the fitted area under the ROC curve. Means were compared by using ANOVA ($P \leq .05$). **Results:** Intraobserver reliability was moderate (0.57 ± 0.22; range, 0.34-0.78). Pan-N (0.72 ± 0.15), CBCT-I (0.65 ± 0.21), and CBCT-S (0.65 ± 0.17) reliability was significantly greater than TOMO (0.44 ± 0.25). The diagnostic accuracy of CBCT-I (0.95 ± 0.05) and CBCT-S (0.77 ± 0.17) was significantly greater than all other modalities (Pan-N [0.64 ± 0.11], Pan-TM [0.55 ± 0.11], TOMO [0.58 ± 0.15]). CBCT-I was also more accurate than CBCT-S, and Pan-N was more accurate than Pan-TM and TOMO. **Conclusions:** CBCT images provide superior reliability and greater accuracy than TOMO and TMJ panoramic projections in the detection of condylar cortical erosion. (Am J Orthod Dentofacial Orthop 2007;132:429-38)

Radiographic imaging is an important diagnostic adjunct in the assessment of an orthodontic patient and occasionally includes specific examinations of the temporomandibular joint (TMJ). Various conditions affecting the TMJ can cause skeletal deformity, malocclusion, masticatory dysfunction, and derangements of the intra-articular disc.[1]

Panoramic, transcranial projections, and tomography are most commonly used in the radiographic assessment of the TMJ in orthodontic practices because of their availability, ease of use, relatively low radiation requirement, and low cost.[1-3] Although many investigators used panoramic radiographs to assess changes in the condyles from functional appliances[4] and other orthodontic treatments,[5,6] the inherent anatomic diversity of the TMJ articulation,[7] compounded by factors that influence 2-dimensional (2D) image presentation[8] (eg, anatomic superimposition, beam projection angle, and patient positional changes), throw into doubt the validity of those studies.

Computed tomography (CT) provides optimal imaging of the osseous components of the TMJ with 87.5%[9] to 96%[10] accuracy in detecting degenerative arthritis. Unfortunately, most traditional CT scanners are large and expensive systems designed for full-body

[a]Graduate student, University of Louisville, Louisville, KY.
[b]Professor, Radiology and Imaging Sciences, Department of Surgical/Hospital Dentistry, University of Louisville School Minnesotal of Dentistry, Louisville, KY.
[c]Private practice, Phoenix, AZ.
[d]Chair, School of Natural Science, Spaulding University, Louisville, KY.
[e]Associate professor, Department of Orthodontics and Pediatric Dentistry, University of Louisville School of Dentistry, Louisville, KY.
[f]Clinical associate professor, Department of Orthodontics and Pediatric Dentistry, University of Louisville School of Dentistry, Louisville, KY.
[g]Professor, Radiology and Imaging Sciences, Department of Surgical/Hospital Dentistry, University of Louisville School of Minnesotal of Dentistry, Louisville, KY.
Reprint requests to: William Charles Scarfe, Radiology and Imaging Sciences, Department of Surgical/Hospital Dentistry, University of Louisville School of Dentistry, 501 S. Preston Street, Louisville, KY 40292; e-mail, wcscar01@gwise.louisville.edu.
Submitted, August 2005; revised and accepted, October 2005.
0889-5406/$32.00

doi:10.1016/j.ajodo.2005.10.032

imaging and not readily available to the orthodontist. CT units can be divided into 2 groups based on acquisition x-ray geometry: fan beam and cone beam. Fan-beam scanners have an x-ray source and detector mounted on a rotating gantry. Data are acquired through a thin, broad, fan-shaped x-ray beam transmitted through the patient. Image production requires reconstructing the patient slice-by-slice and then stacking the slices to obtain a 3-dimensional (3D) representation of the object. Each slice requires a separate scan and separate 2D reconstruction. Cone-beam (CB) CT (CBCT) scanners are based on volumetric tomography, a principle that uses a 2D extended detector and a 3D x-ray beam. This configuration allows for a single rotation of the gantry to generate a scan of the entire region of interest, inherently reducing time for volumetric data acquisition.

Recently, maxillofacial CBCT has been developed specifically for the maxillofacial region.[11-14] At least 4 systems are currently available in the United States: NewTom QR DVT 3G (Quantitative Radiology, Verona, Italy), CB MercuRay (Hitachi Medical, Chibaken, Japan), 3D Accuitomo-XYZ Slice View Tomograph, (J. Morita, Kyoto, Japan), and iCAT (Imaging Sciences International, Hatfield, Pa). Additional manufacturers are poised to introduce commercial units soon. Most CBCT units for maxillofacial applications use an image intensifier tube/charge-coupled device (IIT/CCD), but at least 1 device uses a flat-panel imager (eg, iCAT). The flat-panel detector consists of a cesium-iodide scintillator applied to an amorphous silicon thin-film transistor. Images produced with IIT/CCD generally result in more noise than images from a flat-panel imager and also need to be preprocessed to reduce geometric distortions inherent in the detector configuration. Systems with IIT/CCD configurations might introduce greater measurement inaccuracies, particularly of peripheral structures in the volumetric data set such as the TMJ articulation. Anecdotal discussions with manufacturers indicate that most purchasers of these devices in the United States are specialist dentists, including oral surgeons, periodontists, and orthodontists, followed by dental radiology facilities, both private and institutional.

CBCT can provide submillimeter spatial resolution images with markedly shorter scanning times (10-70 seconds) and has been reported to require somewhat lower radiation dosages than fan-beam or helical CT imaging methods.[12,15-19] Time and dose requirements have been suggested to be of the same order of magnitude as other dental radiographic modalities.[17-19] CBCT allows personal computer-based 2D multi-planar reformatted and secondary reconstruction of the data. This allows the observer to interactively scroll through stacks of submillimeter slices in either conventional display modes (axial, coronal, or sagittal) or multiple transaxial cross-sectional slices.

Maxillofacial applications of CBCT imaging have been reported for oral and maxillofacial surgery[20-24] and implantology,[25-28] and 3D imaging has potential for quantitative craniofacial assessment in orthodontics.[29-34] However, before widespread adoption of this technology, accuracy and efficacy studies are warranted, and the issue of radiation dosage needs further appraisal.

Several authors have reported high dimensional accuracy of maxillofacial CBCT in measuring facial structures,[28,35,36] including the TMJ.[37-41] Tsiklakis et al[37] described a protocol for examining TMJ articulation including transaxial images obtained para-sagittally and para-coronally—ie, in planes parallel or perpendicular to the long axis of the condyle instead of the true anatomic coronal and sagittal planes. They indicated that this series results in high-quality images of the bony components and provided 4 illustrative cases. Although publication involves limited static images to illustrate the diagnoses in these cases, those trained in interpreting volumetric data routinely view sequential and serial slices associated with the region of interest.

Despite descriptions of the application of CBCT to TMJ diagnosis, the comparative accuracy of this modality in the assessment of condylar disease has not been reported. Therefore, this study was performed to compare the diagnostic accuracy of CBCT imaging to conventional TMJ imaging modalities, including panoramic and tomographic radiography, and to evaluate the effect of the viewing mode on the diagnostic efficacy of CBCT.

MATERIAL AND METHODS

This was a blinded observational, in-vitro, cross-sectional study. It was approved by the Institutional Human Remains Committee, Department of Anatomical Sciences and Neurobiology, at the University of Louisville. The initial sample consisted of 80 human skulls. No demographic data were available on them; they were not identified by age, sex, or ethnicity. One author (M.J.H.) took digital photographic images of all TMJ articulations from multiple projections incorporating a #2 forensic MagRule (Arrowhead Scientific, Lenexa, Kan). The condyle on most mandibles was essentially normal morphologically; however, because the specimens are used in teaching, some lateral and medial condylar poles had physical damage, producing cortical defects varying in size. A retrospective visual audit of the photographic records of each TMJ was

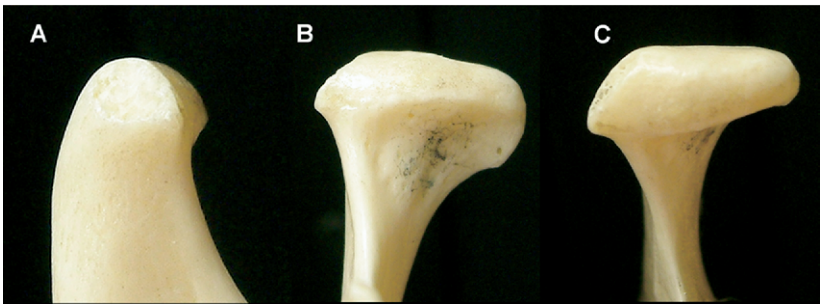

Fig 1. Photographic images of a right TMJ condyle showing erosion of the lateral pole, magnified views: **A,** sagittal; **B,** coronal; **C,** axial.

made by 3 authors (M.J.H., O.B.H., W.C.S.), who reached consensus as to the location and severity of the condylar defects via the Delphi method.[42] Two inclusion criteria were applied to the skulls to provide a subsample with condylar morphologic changes that simulated faceting associated with degenerative osteoarthritic disease. First, only condyles with defects on the lateral pole were included. Then these defects were measured, and only condyles with defects between 5 and 10 mm transversely were selected. The lateral pole was chosen because it is the most common site of condylar deformity in degenerative joint disease (DJD) affecting the TMJ,[43] whereas the size of the lesion was approximately 25% to 50% of the maximum average interpole distance and might be considered moderate-to-severe DJD. Finally, after inspection of the projection images, only condyles that were imaged clearly by all modalities were included. Based on these criteria, a sample of 37 TMJ condyles from 30 skulls was selected; 19 had normal condylar morphology, and 18 had physical defects on the lateral pole simulating moderate-to-severe osteoarthritic changes (Fig 1).

To provide some soft-tissue attenuation, 2 latex balloons filled with water were placed in the cranial vault before imaging. To simulate the TMJ interarticular space and separate the mandibular condyle from the temporal fossa, a 1.5-mm thick foam wedge was placed in the joint space between the glenoid fossa and the condylar head. For all images, the teeth were placed in centric occlusion (maximum intercuspation), and the jaws were held closed with bilateral metal springs. A custom plastic head holder, with a polyvinyl chloride pipe extension for placing into the foramen magnum, was constructed to support the skulls during imaging.

Three modalities were used to image the skulls. CBCT images were acquired with the iCAT unit. The device was operated at 3-8 mA (pulse-mode) and 120 kV by using a high-frequency generator with fixed anode and 0.5 mm nominal focal spot size. The anterior symphyseal region of the mandible of each skull was placed in the chin holder, and vertical and horizontal lasers were used to position the skull. Each specimen was oriented by adjustment of the chin support until the midsagittal plane was perpendicular to the floor and the horizontal laser reference coincided with the intersection of the posterior maxillary teeth and the alveolar ridge. Lateral scout radiographs were taken and small adjustments made so that discrepancies between bilateral structures (eg, posterior and inferior borders of the mandibular rami and zygomatic arches) were less than 5 mm. A single 360° rotation, 20-second scan, comprising 306 basis projections, was then made for each skull with a 17.0 cm (diameter) × 13.2 cm (height) field of view with the iCAT acquisition software (version 1.7.7). Exposure parameters could not be altered because acquisition was controlled by automatic exposure control. Primary reconstruction of the data was automatically performed immediately after acquisition and took approximately 60 seconds. Secondary reconstruction occurred in real time and provided contiguous color-correlated perpendicular axial, coronal, and sagittal 2D multi-planar reformatted slices, resulting in 330 individual 0.4 mm slices in each orthogonal plane. Customized para-coronal 2D reformatting, at 3.6-mm slice thickness localized to the TMJ, was performed with proprietary software, providing a series of 1-mm thick contiguous intercondylar transaxial para-sagittal slices. Nine specific slices were selected to display the entire lateral pole of the condyle and include slices to the middle of the condylar axis. The density and the contrast of the images were adjusted to a standard "bone" window and level (3000/300, respectively). The axial and coronal images were then magnified to 200%, and the cross-sectional pane was increased to display only the axial and coronal images of interest. This provided a standardized magnified display of cross-sectional images (Fig 2). The resultant reference lines and display were then screen

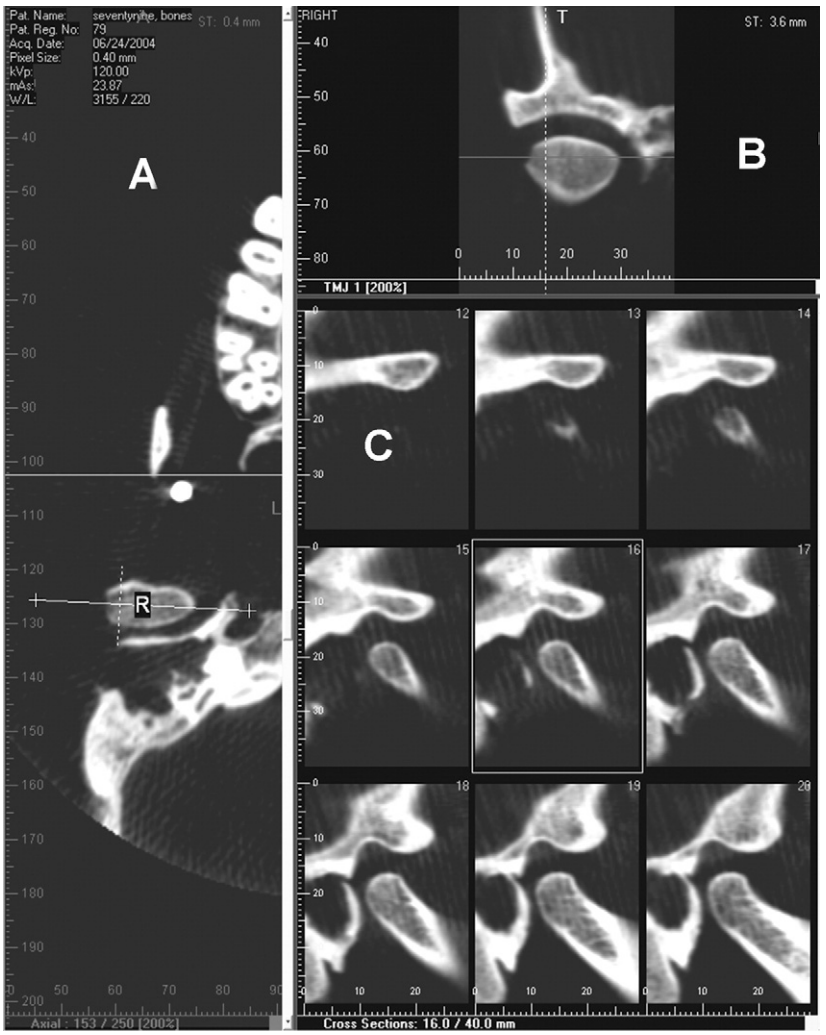

Fig 2. Cropped CBCT TMJ display of right (R) image. Coronal and para-sagittal images of contralateral TMJ not included in study were cropped. **A,** Axial image at the midcondylar level where a line is drawn through the intercondylar axis of both condyles at 200% magnification; **B,** para-coronal reconstruction of TMJ at 200% magnification; **C,** series of para-sagittal 1-mm image slices perpendicular to the intercondylar axis extending medially from the lateral pole.

captured (Snagit, version 7.0; TechSmith, Okemos, Mich) and saved in TIFF format. In addition, the protocol was saved as a patient "map," a proprietary algorithm of the iCAT software that allows retrieval of the protocol when the data are subsequently accessed.

Panoramic images were acquired with the Orthopantomograph OP 100 (Instrumentarium Imaging/GE Medical Systems, Milwaukee, Wis) dental panoramic x-ray machine. The skulls were positioned in the panoramic cephalostat by using the plastic head holder according to the manufacturer's positioning recommendations. Both conventional (Pan-N) and TMJ-specific (Pan-TM) panoramic projections (program 9) of the samples were taken. For Pan-N, the beam projection angle to the TMJ was approximately 30° to the intercondylar axis with a standard focal trough width. This produced a single sagittal oblique image of the condyle with the lateral pole imaged anteriorly (Fig 3). For Pan-TM, the beam projection angle of the TMJ to the intercondylar axis ranged from 0° to 20°, producing wider sagittal and separate posterior focal trough areas limited to the TMJ field. This geometric configuration produces 2 images with the anterior surface imaged anteriorly on the lateral projection and the lateral pole imaged laterally on the posterior anterior image (Fig 4). The submentovertex (SMV) plane projection and linear

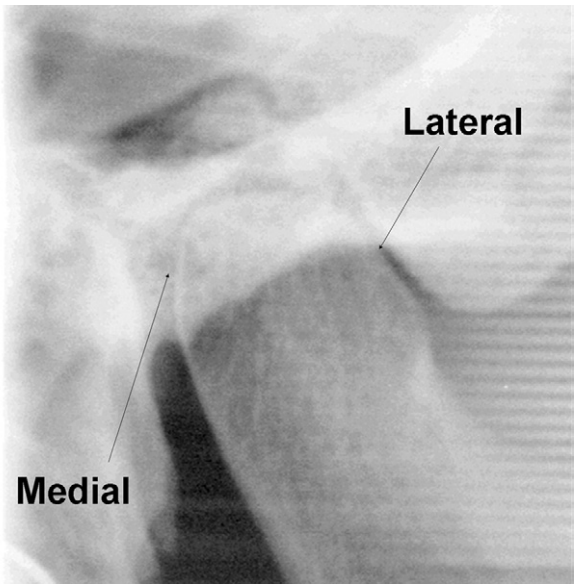

Fig 3. Pan-N cropped image of right condyle with lateral pole defect. The anterior surface of the condylar image is the projected lateral pole.

tomography were performed by using a Quint Sectograph (model QS 10-1627W; Denar, Anaheim, Calif). A narrow reference slice (2 mm) corrected para-sagittal image was taken at the midpoint of the axis distance of each condyle (central cut) and at 7 mm medially (medial cut) and laterally (lateral cut) to this location. In addition, a single medium slice para-coronal image of the condyle was taken (Fig 5).

Panoramic and tomographic images were acquired by using 6 × 12-in and 8 × 10-in photostimulable storage phosphor imaging plates, respectively. Exposure parameters for each technique were determined by subjective evaluation of the image quality of many images at various exposures taken on a skull with a 1-cm thick polymethyl methacrylate acrylic attenuation material over the exit beam. The plates were scanned at 300 dpi and saved as 16-bit TIFF files by using the DenOptix imaging system (Gendex/Kavo, Des Plaines, Ill). The images were equalized and despeckled with proprietary software (VixWin 2000, version 1.2; Gendex/Kavo) before export as 8-bit TIFF images. CBCT images were acquired with a megapixel (1024 × 1024 matrix) flat-panel hydrogenated amorphous silicon detector with a cesium-iodide scintillator and stored as DICOM files. CB reconstructed images were reformatted from 306 projections, providing a pixel matrix size of 0.4 mm.

To be able to display the digital images localized to the condyles on the monitor at actual size, regions of interest of various sizes centered on the mandibular condyle were cropped from the panoramic, SMV, and tomographic images by using PhotoShop software (version 7.0; Adobe Systems, San Jose, Calif). Although the Pan-N images could be displayed 1 at a time, it was necessary to create an image montage with PhotoShop for modalities to show the condyle in various projections. For Pan-TM, a cropped montage of para-sagittal and para-coronal images was displayed (Fig 4). For corrected angle linear tomography (TOMO), cropped para-sagittal and coronal cross-sectional images and cropped SMV axial images were displayed (Fig 5). For the CBCT images, a static screen capture of the TMJ patient "map" was presented (Fig 2) with the pane showing the contralateral TMJ blacked out (CBCT-S). Image montages were created on a canvas of 1600 × 1200 matrix size and saved as TIFF images. Screen capture of the CBCT-S was performed on the viewing monitor at the same matrix size. The images were coded, randomized, and presented with 10 duplicate images (5 control, 5 with defects) as a slide show at a captured-to-monitor ratio of 1:1 with no time limitation by using IrfanView (version 3.97, Irfan Skiljan, Wiener Neustadt, Austria). Ten dentists with varying expertise in viewing TMJ images acted as observers. Two observers were oral and maxillofacial radiologists, 1 was a TMJ pain specialist, 2 were general practitioners, 2 were orthodontists, and 3 were orthodontic residents in their last year of training. All had some experience in TMJ interpretation, except for the radiologists, who were experienced in the interpretation CBCT images. The observers viewed the slide show on a 20.1-in flat-panel thin-film transistor color monitor (Flexscan L885; Eizo Nanao, Ishikawa, Japan) with a screen resolution of 1600 × 1200 and a 0.255 × 0.255 mm pixel pitch operated at 32-bit. In addition, in a separate CBCT session, the observers were allowed to interact with the display by scrolling the axial and para-sagittal image slices (CBCT-I).

The observers had an orientation session and a visual instruction sheet to assist in identifying the appropriate surface. They were then asked to evaluate the lateral surface of the condyle of the mandible and rate their confidence about the presence or absence of a defect using the following scale: (1) definitely present, (2) probably present, (3) unsure, (4) probably absent, and (5) definitely absent. The observers received detailed instructions defining that a condylar defect demonstrated either (1) faceting—a small, smooth, flat surface or irregularity seen on the bony outline of the condyle producing a sharp deviation in condylar form; (2) lack of cortical definition—loss of peripheral

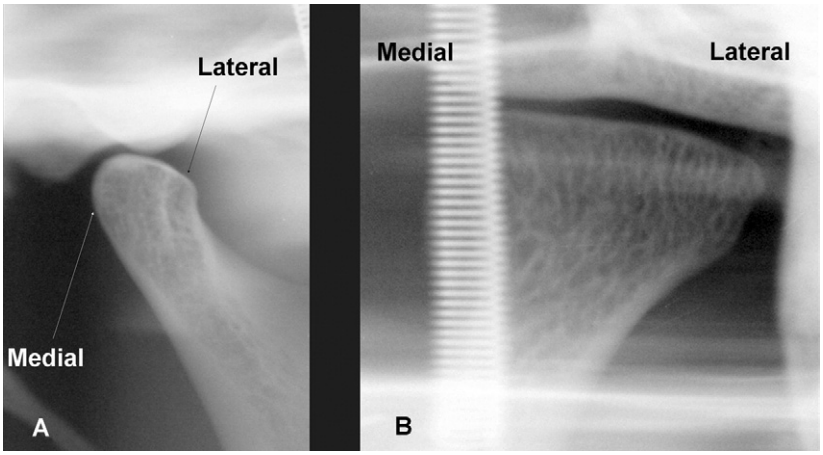

Fig 4. Pan-TM cropped images of same condyle as in Figure 3. **A,** Lateral corrected cross-sectional; **B,** magnified wide-slice posteroanterior coronal projection. The location of the lateral pole is shown.

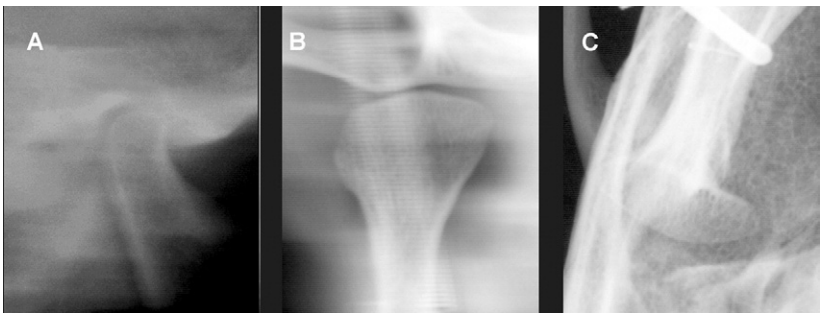

Fig 5. TOMO cropped images of same condyle as in Figure 3. **A,** Corrected angle lateral (para-sagittal) tomogram; **B,** corrected angle frontal (para-coronal) tomogram; **C,** cropped magnified axial (SMV) image.

opaque rim of cortical bone; or (3) both faceting and lack of cortical contour.

Statistical analysis

All data were entered into Excel 2003 (Microsoft, Redmond, Wash). The diagnostic accuracy of each observer and each mode was compared with the true diagnosis (anatomy) by calculating the sensitivity and 1-specificity values; this is presented as receiver operating characteristic (ROC) curve areas. The averages of the diagnostic performances of the 10 observers were used to generate an average ROC curve for each imaging mode.[44] Differences between the areas under the ROC curves were assessed by using analysis of variance (ANOVA) at the 95% significance level. The weighted kappa values were computed as a measure of intraobserver variability and interpreted according to the criteria of Landis and Koch[45]: 0.81 (very good or excellent), 0.61-0.80 (good or substantial), 0.41-0.60 (moderate), 0.21-0.40 (fair), and 0.20 (poor) agreement.

RESULTS

The kappa values for intraobserver agreement ranged from 0.35 (observer H) to 0.79 (observer J) (Table I). Two observers had fair agreement, 4 had moderate agreement, and 4 had substantial agreement with their own scorings. The average intraobserver kappa value was 0.57 $\pm$ 0.22. There were significant differences between observers ($F = 2.4$, $P = .028$); observer H was more unreliable than 6 other observers (A, B, C, E, I, and J). Significant differences were also observed between modalities ($F = 3.11$, $P = .024$). Both CBCT modes (I and S) and Pan-N were significantly more reliable than TOMO ($t = -2.68$, $P = .025$; $t = 2.6$, $P = .029$; and $t = 3.13$, $P = .012$, respectively).

Table I. Intraobserver reliability: kappa (κ_w) for 10 observers of each of 5 imaging modalities in the detection of cortical erosive defects of the mandibular condyle lateral pole

	CBCT		*Panoramic*			
Observer	*Interactive*	*Static*	*Normal*	*TMJ*	*Tomography*	*Mean ± SD*
A	0.742	0.778	0.667	0.492	0.224	0.580 ± 0.228
B	0.837	0.643	0.776	0.717	0.859	0.766 ± 0.089
C	0.621	0.643	0.906	0.734	0.706	0.722 ± 0.112
D	0.556	0.489	0.524	0.662	0.483	0.543 ± 0.073
E	0.851	0.789	0.940	0.338	0.308	0.645 ± 0.299
F	0.353	0.692	0.546	0.444	0.444	0.496 ± 0.129
G	0.489	0.432	0.744	−0.125	0.405	0.389 ± 0.317
H	0.412	0.375	0.702	0.286	−0.026	0.350 ± 0.261
I	0.706	0.808	0.808	0.216	0.444	0.596 ± 0.259
J	1.000	0.898	0.552	0.894	0.583	0.785 ± 0.204
Mean ± SD	0.657 ± 0.208	0.655 ± 0.174	0.716 ± 0.147	0.466 ± 0.247	0.443 ± 0.208	0.57 ± 0.22

One-way ANOVA, F = 3.11, P = .24.
Post-hoc analysis: the intraobserver reliability of both CBCT modes and Pan-N is statistically greater than TOMO (CBCT-I, P = .012; CBCT-S, P = .028; Pan-N, P = .012).

Table II. Diagnostic accuracy of 10 observers using 5 modalities to detect erosive cortical defects of the mandibular condyle lateral pole: fitted area under the ROC curve

	CBCT		*Panoramic*			
Observer	*Interactive*	*Static*	*Normal*	*TMJ*	*Tomography*	*Mean ± SD*
A	0.962	0.830	0.555	0.778	0.798	0.784 ± 0.147
B	0.954	0.904	0.529	0.484	0.648	0.704 ± 0.215
C	0.849	0.493	0.659	0.581	0.589	0.634 ± 0.134
D	0.938	0.529	0.548	0.559	0.399	0.595 ± 0.202
E	0.937	0.610	0.687	0.519	0.631	0.677 ± 0.158
F	0.975	0.887	0.812	0.582	0.530	0.757 ± 0.193
G	1.000	0.789	0.534	0.348	0.423	0.619 ± 0.271
H	0.936	0.858	0.802	0.478	0.559	0.727 ± 0.198
I	1.000	0.901	0.699	0.625	0.801	0.805 ± 0.151
J	0.914	0.942	0.616	0.500	0.384	0.671 ± 0.249
Mean ± SD	0.946 ± 0.044	0.774 ± 0.167	0.644 ± 0.106	0.545 ± 0.112	0.576 ± 0.150	

One-way ANOVA, F = 17.85, P <.00001.
Post-hoc analysis: CBCT-I is statistically more accurate than Pan-N (P <.0001), Pan-TM (P <.0001), TOMO (P <.0001), and CBCT-S (P <.0048).
CBCT-S is statistically more accurate than Pan-N (P = .05), Pan-TM (P = .0062), and TOMO (P = .013).
Pan-N is statistically more accurate than Pan-TM (P = .0063) and TOMO (P = .013).

The area under the ROC curve for each observer in the assessment of lateral condylar pole defects varied according to the imaging mode (Table II). The diagnostic accuracies of CBCT-I (0.95 ± 0.05) and CBCT-S (0.77 ± 0.17) were significantly greater than all other modalities (Pan-N [0.64 ± 0.11], Pan-TM [0.55 ± 0.11], TOMO [0.58 ± 0.15]). CBCT-I was also more accurate than CBCT-S, and Pan-N was more accurate than Pan-TM and TOMO. The means of the ROC area for each observer over 5 imaging modes ranged from 0.6 (observer D) to 0.81 (observer I). Comparison of these means between observers provided a measure of interobserver reliability. There were no statistically significant differences between the observers (F = 0.43, P = .91).

DISCUSSION

No single imaging technique has been readily available to orthodontists for accurate, easily interpreted representations of all osseous aspects of the TMJ complex and associated structures. Previously, conventional plane projections such as the panoramic, modified TMJ-specific panoramic, transcranial, and, to a lesser extent, Townes and SMV have been used, usually combined to provide an appreciation of TMJ anatomy. Cross-sectional tomographic imaging, either

limited slice film-based or computed, has been used in TMJ evaluation; however, financial and radiation dose costs, as well as access, inherently limit the routine use of these modalities in orthodontics. The recent introduction of dentomaxillofacial CBCT equipment and the rapidly emerging availability of this technology now give clinicians the capability of reformatting the volumetric data set to provide conventional (eg, panoramic and "sum ray" wide-slice sections simulating plane projections such as cephalometric, SMV, and posteroanterior views) and cross-sectional (eg, para-sagittal and para-coronal) imaging—all after 1 exposure scan. This potentially provides improved clinical efficacy at a similar or a lower cost than conventional combination imaging (panoramic, cephalometric, and TMJ imaging).

The purpose of this investigation was to compare the diagnostic accuracy of CBCT, 2 modes of panoramic radiography, and tomography in detecting simulated defects on the lateral pole of the mandibular condyle. We found the intraobserver reliability of CBCT images were substantially greater than plane projection linear tomography. In addition, we found CBCT images to provide significantly greater accuracy than tomography and TMJ-specific panoramic projections in the detection of simulated condylar defects. This result was expected because CBCT display of TMJ volumetric data provides multiple para-sagittal 1-mm slices of high contrast with no structural superimposition or tomographic blur, as do the other images. Interestingly, we did not find improved accuracy for detecting TMJ defects using TMJ-specific panoramic modes. This might be related to the observers' unfamiliarity with images produced by this modality or the inherent superimposition of structures, variable distortion, and the wide focal trough of this modality.

CBCT data were presented to observers in 2 formats. CBCT-S images were used as analogous to single panoramic and limited slice tomographic images. We found that the ability to interact with the CBCT data display by scrolling through contiguous slices of either axial or para-sagittal images provided a significant (20%) improvement in accuracy compared with the interpretation of CBCT-S images. This improvement was realized for all observers, regardless of experience. It suggests that CBCT data can only be appropriately interpreted by access to the volumetric data set.

This study was limited in that the defects on the lateral poles of this sample might not be an appropriate representation of DJD of the TMJ. Osteoarthritis of the mandibular condyle not only produces flattening of the surface, as simulated by the defect, but might also be associated with morphologic and surface changes such as sclerosis, osteophyte formation, and reduced interarticular space. Although the potential sample size for this study was large, many condyles were excluded because they were inadequately shown on at least 1 of the 3 plane projections. Most commonly, this was due to superimposition of the springs attaching the mandible to the cranium on the region of interest, a problem inherent in anatomical specimens that is not consequential in actual clinical imaging. We originally also imaged all condyles using transcranial radiography. However, we did not include these images in the study design because superimposition of the metallic springs substantially reduced the number of image sets. Our access to the sample was time limited, and we could not reimage the condyles or remove the springs.

Similar comparative studies should be performed on patients with DJD of the TMJ to demonstrate the full spectrum of TMJ articular dysmorphology and determine wheither the accuracy of CBCT remains high; however, this could be considered unethical because of the radiation from the many exposures that would be required. Although conventional CT provides high accuracy, limitations exist in the depiction of TMJ surfaces less than 1-mm thick; accuracy depends on the orientation of scanning planes being less than 35° to the orbito-meatal plane.[46] CBCT data acquisition is generally isotropic and therefore less susceptible to partial-volume averaging effects in this region.[40] Further studies should investigate the effect of varying skull position on diagnostic accuracy. In addition, clinical cost-benefit analyses should be performed to assist in developing appropriate patient selection criteria for CBCT imaging in evaluating TMJ disease.

CONCLUSIONS

CBCT images provide superior reliability and greater accuracy than corrected angle linear tomography and TMJ panoramic projections in the detection of condylar cortical erosion.

REFERENCES

1. Brooks SL, Brand JW, Gibbs SJ, Hollender L, Lurie AG, Omnell KA, et al. Imaging of the temporomandibular joint: a position paper of the American Academy of Oral and Maxillofacial Radiology. Oral Surg Oral Med Oral Pathol Oral Radiol Endod 1997;83:609-18.
2. Katzberg RW. State of the art: temporomandibular joint imaging. Ann Royal Aust Coll Dent Surg 1989;10:2-52.
3. Dixon D. Radiographic diagnosis of temporomandibular disorders. In: Sadowsky PL, Laskin DM, editors. Seminars in orthodontics: temporomandibular joint disorders: fact or fiction. Philadelphia: W. B. Saunders; 1995. p. 207-21.
4. Uematsu H, Ichida T, Masumi S, Morimoto Y, Tanaka T, Konoo T, et al. Diagnostic image analyses of activator treated temporo-

mandibular joint in growth and maturing stages. Cranio 2002;20:254-63.
5. Peltola JS, Kononen M, Nystrom M. A follow-up study of radiographic findings in the mandibular condyles of orthodontically treated patients and associations with TMD. J Dent Res 1995;74:1571-6.
6. Carlton KL, Nanda RS. Prospective study of posttreatment changes in the temporomandibular joint. Am J Orthod Dentofacial Orthop 2002;122:486-90.
7. Solberg WK, Hansson TL, Nordstrom B. The temporomandibular joint in young adults at autopsy: a morphologic classification and evaluation. J Oral Rehabil 1985;12:303-21.
8. McDavid WD, Tronje G, Welander U, Morris CR. Dimensional reproduction in rotational panoramic radiography. Oral Surg Oral Med Oral Pathol 1986;62:96-101.
9. Westesson PL, Katzberg RW, Tallents RH, Sanchez-Woodworth RE, Svensson SA. CT and MR of the temporomandibular joint: comparison with autopsy specimens. AJR Am J Roentgenol 1987;148:1165-71.
10. Manzione JV, Katzberg RW, Brodsky GL, Seltzer SE, Mellins HZ. Internal derangements of the temporomandibular joint: diagnosis by direct sagittal computed tomography. Radiology 1984;150:111-5.
11. Mozzo P, Procacci C, Tacconi A, Martini PT, Andreis IA. A new volumetric CT machine for dental imaging based on the cone-beam technique: preliminary results. Eur Radiol 1998;8:1558-64.
12. Hashimoto K, Arai Y, Iwai K, Araki M, Kawashima S, Terakado M. A comparison of a new limited cone beam computed tomography machine for dental use with a multidetector row helical CT machine. Oral Surg Oral Med Oral Pathol Oral Radiol Endod 2003;95:371-7.
13. Sukovic P. Cone beam computed tomography in craniofacial imaging. Orthod Craniofac Res 2003;6(Suppl 1):31-6.
14. Baba R, Ueda K, Okabe M. Using a flat-panel detector in high resolution cone beam CT for dental imaging. Dentomaxillofac Radiol 2004;33:285-90.
15. Bianchi S, Anglesio S, Castellano S, Rizzi L, Ragona R. Absorbed doses and risk in implant planning: comparison between spiral CT and cone-beam CT [abstract]. Dentomaxillofac Radiol 2001;30(Suppl 1):S28.
16. Schulze D, Heiland M, Thurmann H, Adam G. Radiation exposure during midfacial imaging using 4- and 16-slice computed tomography, cone beam computed tomography systems and conventional radiography. Dentomaxillofac Radiol 2004;33:83-6.
17. Ludlow JB, Davies-Ludlow LE, Brooks SL. Dosimetry of two extraoral direct digital imaging devices: NewTom cone beam CT and Orthophos Plus DS panoramic unit. Dentomaxillofac Radiol 2003;32:229-43.
18. Mah JK, Danforth RA, Bumann A, Hatcher D. Radiation absorbed in maxillofacial imaging with a new dental computed tomography device. Oral Surg Oral Med Oral Pathol Oral Radiol Endod 2003;96:508-13.
19. Tsiklakis K, Donta C, Gavala S, Karayianni K, Kamenopoulou V, Hourdakis CJ. Dose reduction in maxillofacial imaging using low dose Cone Beam CT. Eur J Radiol 2005;56:413-7.
20. Ziegler CM, Woertcher R, Brief J, Hassfeld S. Clinical indications for digital volume tomography in oral and maxillofacial surgery. Dentomaxillofac Radiol 2002;31:126-30.
21. Nakagawa Y, Kobayashi K, Ishii H, Mishima A, Ishii H, Asada K, et al. Preoperative application of limited cone beam computerized tomography as an assessment tool before minor oral surgery. Int J Oral Maxillofac Surg 2002;31:322-6.
22. Danforth RA, Peck J, Hall P. Cone beam volume tomography: an imaging option for diagnosis of complex mandibular third molar anatomical relationships. J Calif Dent Assoc 2003;31:847-52.
23. Heiland M, Schmelzle R, Hebecker A, Schulze D. Intra-operative 3D imaging of the facial skeleton using the SIREMOBIL Iso-C3D. Dentomaxillofac Radiol 2004;33:130-2.
24. Hamada Y, Kondoh T, Noguchi K, Iino M, Isono H, Ishii H, et al. Application of limited cone beam computed tomography to clinical assessment of alveolar bone grafting: a preliminary report. Cleft Palate Craniofac J 2005;42:128-37.
25. Hatcher DC, Dial C, Mayorga C. Cone beam CT for pre-surgical assessment of implant sites. J Calif Dent Assoc 2003;31:825-33.
26. Sarment DP, Sukovic P, Clinthorne N. Accuracy of implant placement with a stereolithographic surgical guide. Int J Oral Maxillofac Implants 2003;18:571-7.
27. Sato S, Arai Y, Shinoda K, Ito K. Clinical application of a new cone-beam computerized tomography system to assess multiple two-dimensional images for the preoperative treatment planning of maxillary implants: case reports. Quintessence Int 2004;35:525-8.
28. Kobayashi K, Shimoda S, Nakagawa Y, Yamamoto A. Accuracy in measurement of distance using limited cone-beam computerized tomography. Int J Oral Maxillofac Implants 2004;19:228-31.
29. Mah JD, Hatcher D. Current status and future needs in craniofacial imaging. Orthod Craniofac Res 2003;6(Suppl 1):10-6.
30. Vannier MW. Craniofacial computed tomography scanning: technology, applications and future trends. Orthod Craniofac Res 2003;6(Suppl 1):23-30.
31. Maki K, Inou N, Takanishi A, Miller AJ. Computer-assisted simulations in orthodontic diagnosis and the application of a new cone beam x-ray computed tomography. Orthod Craniofac Res 2003;6(Suppl 1):95-101.
32. Baumrind S, Carlson S, Beers A, Curry S, Norris K, Boyd RL. Using three-dimensional imaging to assess treatment outcomes in orthodontics: a progress report from the University of the Pacific. Orthod Craniofac Res 2003;6(Suppl 1):132-42.
33. Aboudara CA, Hatcher D, Nielsen IL, Miller A. A three-dimensional evaluation of the upper airway in adolescents. Orthod Craniofac Res 2003;6(Suppl 1):173-5.
34. Danforth RA, Dus I, Mah J. 3-D volume imaging for dentistry: a new dimension. J Calif Dent Assoc 2003;31:817-23.
35. Lascala CA, Panella J, Marques MM. Analysis of the accuracy of linear measurements obtained by cone beam computed tomography (CBCT-NewTom). Dentomaxillofac Radiol 2004;33:291-4.
36. Marmulla R, Wortche R, Muhling J, Hassfeld S. Geometric accuracy of the NewTom 9000 Cone Beam CT. Dentomaxillofac Radiol 2005;34:28-31.
37. Tsiklakis KK, Syriopoulos K, Stamatakis HC. Radiographic examination of the temporomandibular joint using cone beam computed tomography. Dentomaxillofac Radiol 2004;33:196-201.
38. Beason R, Brooks SL. TMJ imaging accuracy using alpha prototype of DentoCAT™cone-beam CT [abstract]. J Dent Res 2004;83(Spec Iss A):1938.
39. Honda K, Arai Y, Kashima M, Takano Y, Sawada K, Ejima K, et al. Evaluation of the usefulness of the limited cone-beam CT (3DX) in the assessment of the thickness of the roof of the glenoid fossa of the temporomandibular joint. Dentomaxillofac Radiol 2004;33:391-5.
40. Honda K, Larheim TA, Johannessen S, Arai Y, Shinoda K, Westesson PL. Ortho cubic super-high resolution computed

tomography: a new radiographic technique with application to the temporomandibular joint. Oral Surg Oral Med Oral Pathol Oral Radiol Endod 2001;91:239-43.

41. Hilgers ML, Scarfe WC, Scheetz JP, Farman AG. Accuracy of linear temporomandibular joint measurements with cone beam computed tomography and digital cephalometric radiography. Am J Orthod Dentofacial Orthop 2005;128: 803-11.
42. Stheeman SE, van 't Hof MA, Mileman PA, van der Stelt PF. Use of the Delphi technique to develop standards for quality assessment in diagnostic radiology. Community Dent Health 1995;12:194-9.
43. Solberg WK, Hansson TL, Nordstrom B. The temporomandibular joint in young adults at autopsy: a morphologic classification and evaluation. J Oral Rehabil 1985;12:303-21.
44. DeLong ER, DeLong DM, Clarke-Pearson DL. Comparing the areas under two or more correlated receiver operating curves. A nonparametric approach. Biometrics 1988;44:837-45.
45. Landis JR, Koch GG. An application of hierarchical kappa-type statistics in the assessment of majority agreement among multiple observers. Biometrics 1977;33:363-74.
46. Ahlqvist JB, Isberg AM. Validity of computed tomography in imaging thin walls of the temporal bone. Dentomaxillofac Radiol 1999;28:13-9.